

Fluctuations of the multiplicity of produced particles in onium-nucleus collisions

Tseh Liou¹, A. H. Mueller¹, S. Munier²

¹ *Department of Physics, Columbia University, New York, USA*

² *Centre de Physique Théorique, École Polytechnique, CNRS, Université Paris-Saclay, Palaiseau, France.*

August 3, 2016

Abstract

We address the general features of event-by-event fluctuations of the multiplicity of gluons produced in the scattering of a dilute hadron off a large nucleus at high energy in the fragmentation region of the dilute hadron. We relate these fluctuations to the stochasticity of the number of quanta contained in the hadron at the time of the interaction. For simplicity, we address the ideal case in which the hadron is an onium, and investigate different kinematical regimes in rapidity and onium size. We show that at large rapidity, the multiplicity distribution exhibits an exponential tail in the large-multiplicity region, which is qualitatively consistent with the proton-nucleus data. But interestingly enough, the exponential shape is determined by confinement.

1 Introduction

The large amount of data collected at the RHIC and at the LHC has made accessible the study of event-by-event fluctuations of a number of measurable quantities, such as particle multiplicities in proton-nucleus and nucleus-nucleus collisions. The microscopic origin of the observed stochasticity is however not clear, and various interpretations and phenomenological models have been proposed.

In the available models to date, the stochasticity is often correlated to the event-by-event fluctuations of the matter density in the nucleus. (For a recent review on quantum fluctuations in the initial state of heavy-ion collisions, see e.g. [1]). A common assumption is that the nucleus is a set of nucleons whose positions in the transverse plane relative to its center are random, see for example the PHOBOS Glauber Monte Carlo model [2]. The flow of particles which go to the final state is then related to the geometry of the initial nucleus.

Other recent models assume that the density of gluons significantly fluctuates from nucleon to nucleon, and that these fluctuations are encoded in the large-rapidity fluctuations of the saturation scale [3]. However, such effects were shown, theoretically [4] as well as phenomenologically [5], to be small at realistic collider energies.

In this paper, we investigate the assumption that the fluctuations of the multiplicity of the produced particles in the forward rapidity region of the proton in proton-nucleus collisions is entirely due to the event-by-event fluctuations of the gluon content in the proton generated by the small- x evolution, which are known to be large (see e.g. the recent work of Ref. [6]). The

nucleus is instead a non-fluctuating object. Indeed, we observe that generally speaking, it is quite unnatural to have configurations of nucleons inside the nucleus which are very different from uniformly distributed since the wavefunction of a large nucleus is approximately the same as the ground-state wavefunction of nuclear matter, for which it is known that density fluctuations are very small [7].

Our paper is organized as follows. In the next section, we expose our picture of multiplicity fluctuations, relating them to the parton number fluctuations in the initial state of the dilute object. In Sec. 3, we provide the necessary background on small- x evolution in the Balitsky-Fadin-Kuraev-Lipatov (BFKL) [8, 9, 10] regime, and in particular, we rederive the set of equations obeyed by the moments of the gluon number in the framework of the color dipole model [11]. In Sec. 4, we review the collinear, or double-logarithmic (DL) limit of these equations, relevant when the rapidity is large compared to the logarithm of the ratio of the relevant transverse scales, and solve them to obtain the multiplicity distribution. In Sec. 5, we release the DL approximation: The result of this plain BFKL calculation will prove unphysical, a problem that we shall address in the subsequent section 6. The concluding section contains some prospects, while two appendices discuss small- x evolution in the diffusive approximation (Appendix A), and a numerical study of a dimensionally-reduced model which should share the main features of the full BFKL evolution (Appendix B).

2 Picture of the multiplicity fluctuations

As announced in the Introduction, we shall concentrate on particle production in onium-nucleus collisions in the fragmentation region of the onium. We will argue that in this process, the shape of the multiplicity distribution in a specific kinematical region that we shall define properly below can be traced back to the fluctuations of the *number of quanta* in the wavefunction of the onium at the time of its interaction with the nucleus [12]. Our aim is not to build a realistic model for real hadron-nucleus scattering, but rather to study in as many details as possible onium (namely dipole)-nucleus scattering and derive, in this simple case, the distribution of the number of particles (actually gluons) in the final state. We expect that the main characteristics of the distribution we will find go over unchanged to the experimentally measurable proton-nucleus or deuterium-nucleus scattering processes.

This very kind of statistical fluctuations of the partonic content of hadrons has been considered before: Their impact on the shape and energy evolution of deep-inelastic scattering cross sections was investigated in the deep saturation regime [13] and at more moderate energies [14] (for reviews, see [15, 16]). Here, we consider the effect of these fluctuations on a final-state observable.

Throughout our work, the nucleus will be characterized by one single momentum scale $Q_s(y_0) \gg \Lambda_{\text{QCD}}$, its saturation scale, which depends on its rapidity y_0 in the considered frame (see Fig. 1). The latter scale just sets the upper bound on the transverse momentum of the gluons in the onium wavefunction that are freed and go to the final state.

Indeed, for an onium moving along the positive z axis of a frame in which it has the lightcone momentum p_+ and in the corresponding $A_+ = 0$ gauge, particles are produced as follows:¹ Gluons in the wavefunction of the initial onium that have a transverse momentum smaller than the saturation momentum of the nucleus undergo multiple scatterings with the nucleus and

¹See e.g. Ref. [17] for a good review on high-energy scattering and on particle production

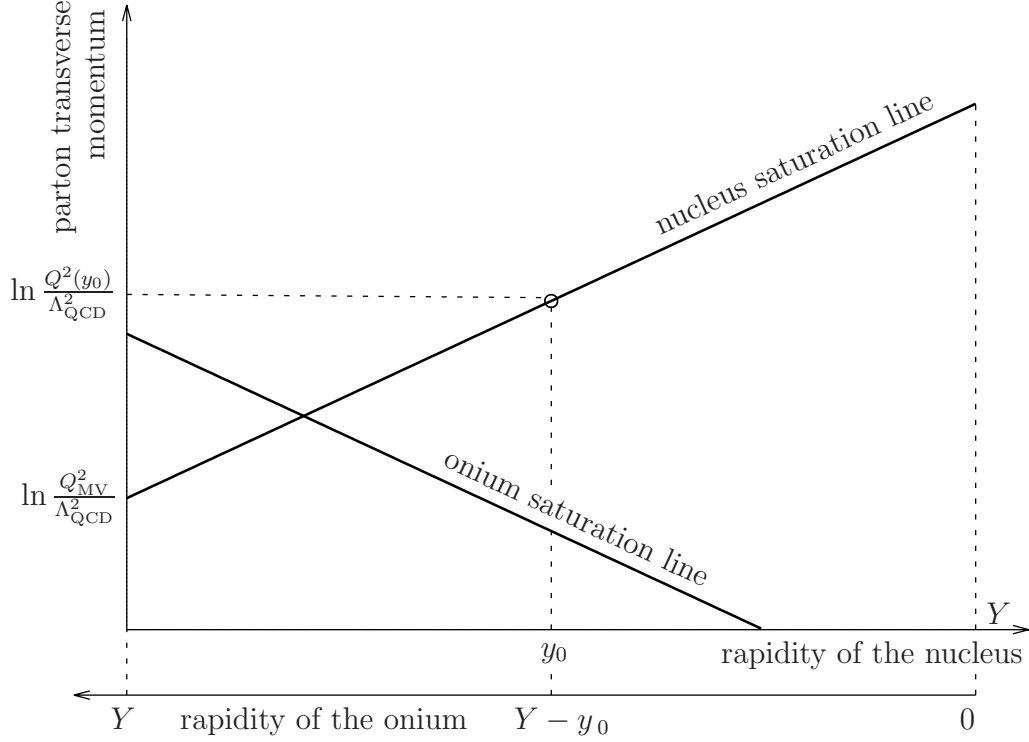


Figure 1: Kinematics of onium-nucleus scattering at fixed total rapidity Y . The rapidity of the nucleus (x -axis) defines the frame. The saturation lines of the onium and of the nucleus are shown. We choose a frame, in which the nucleus has the rapidity y_0 along the negative z axis, such that the onium is a dilute object for gluons of transverse momenta of the order of the saturation scale of the nucleus: The rapidity dependence of its gluon content is then given by the small- x gluon branching process without saturation effects.

are freed, while the nucleus will essentially be transparent to gluons with transverse momenta larger than the nuclear saturation scale. The mean multiplicity of the produced gluons per unit rapidity measured at central rapidity $y \simeq 0$ is related to the distribution $xG(x, Q_s^2(y_0))$ of gluons in the onium of lightcone momentum $k_+ = xp_+$ integrated up to the transverse momentum scale $Q_s(y_0)$ as follows² [18, 19]:

$$\left. \frac{dN}{dy} \right|_{y \simeq 0} = xG(x, Q_s^2(y_0)) \ , \quad \text{where} \quad x = e^{y_0} \frac{Q_s(y_0)}{\sqrt{2}p_+}. \quad (1)$$

Formula (1) relates expectation values, namely mean quantities, where the averages are taken over events. In a given event, just before the collision occurs, the incoming onium is found in a particular Fock state (essentially made of gluons if its rapidity is large enough). The number of gluons and their momenta are random variables whose values fluctuate from event to event. We are going to assume that an equation similar to Eq. (1) holds as an identity between the *random variables* “number of produced particles per unit rapidity in the particular considered event” and “number of gluons in the corresponding realization of the quantum evolution of the onium”. Then the distribution of the multiplicity of particles produced is tantamount to the distribution

² $x = k_+/p_+ = [k_+\sqrt{2}/Q_s(y_0)] \times [Q_s(y_0)/\sqrt{2}p_+] = \sqrt{k_+/k_-} \times Q_s(y_0)/\sqrt{2}p_+$, where the last equality stems from the mass-shell condition $2k_+k_- = Q_s^2(y_0)$. The first factor is then the exponential of the rapidity of the measured gluon relative to the rapidity of the nucleus, namely e^{y_0} .

An equivalent formula is $x = e^{-(Y-y_0)}Q_s(y_0)/M$, where M is the mass of the onium.

of the gluon number in the particular realization of the partonic content of the onium at the time of its interaction with the nucleus.

We will choose the frame (namely the rapidity y_0 of the nucleus) in such a way that the onium (which has the rapidity $Y - y_0$) appears as a dilute object whose state develops through a (linear) branching process, while the nucleus is characterized by a large saturation scale $Q_s(y_0) \gg \Lambda_{\text{QCD}}$, see Fig. 1. In the next section, we shall review small- x evolution in the linear regime.

3 Background on the small- x evolution in the linear regime

Throughout, we will use the large number-of-color limit which will enable us to always represent the partonic content of the onium by a set of color dipoles [11].

We consider the set of dipoles generated by small- x evolution starting with a dipole of size x_{01} , which is our initial condition. Our goal in this paper amounts to computing the probability to observe a number $n(r_s; x_{01}, y)$ of dipoles of size larger than r_s at some rapidity y in one event, starting the evolution from a single dipole.

At double logarithmic accuracy³, there is a simple relation between the ordinary (namely integrated) gluon density that appears in Eq. (1) and the first moment of n :

$$xG(x, Q_s^2(y_0)) = \frac{\partial}{\partial y} n^{(1)}(r_s = 1/Q_s(y_0); x_{01}, y) \Big|_{y=\ln 1/x}, \quad (2)$$

where $n^{(1)}$ is the dipole number averaged over the events: $n^{(1)} = \langle n \rangle$. We shall assume that this relation would also hold as an identity between the gluon density and the rate of evolution of the dipole number with the rapidity *in each realization* of the quantum evolution.

We start by discussing the QCD evolution in the dipole model. Then, we establish the evolution equations for the dipole number.

3.1 QCD evolution and dipole branching

The QCD evolution results from the branching of the dipoles when the longitudinal phase space opens, namely when the rapidity grows. This branching is due to the emission of a gluon at position \mathbf{x}_2 in the transverse plane from one of the endpoints of the dipoles, at respective positions \mathbf{x}_0 and \mathbf{x}_1 . The rate of emission, per unit rapidity dy and transverse surface $d^2\mathbf{x}_2$, is given by the BFKL kernel

$$K_0(\mathbf{x}_2; \mathbf{x}_0, \mathbf{x}_1) = \frac{\bar{\alpha}}{2\pi} \frac{x_{01}^2}{x_{02}^2 x_{12}^2}, \quad (3)$$

where $x_{ij} = |\mathbf{x}_i - \mathbf{x}_j|$ is the size of the corresponding dipole. If one is not interested in the absolute position of the dipoles in the transverse plane but only in their sizes, then it is useful to express this rate as a rate of emission per unit size and rapidity:

$$K(x_{02}, x_{12}; x_{01}) = \bar{\alpha} \frac{4x_{01}^2}{x_{02}x_{12}} \frac{1}{\sqrt{[(x_{12} + x_{02})^2 - x_{01}^2] [x_{01}^2 - (x_{12} - x_{02})^2]}}. \quad (4)$$

This formula holds whenever the distances x_{01} , x_{02} and x_{12} may represent the length of the edges of a triangle, and $K = 0$ if this condition is not verified. $K(x_{02}, x_{12}; x_{01})dx_{02}dx_{12}dy$ is

³The most straightforward way to check Eq. (2) is to compare the explicit expressions its left and right-hand sides. In the double-log approximation, the gluon density xG reads $xG(x, Q^2) = \sqrt{\bar{\alpha} \ln Q^2/y} I_1(2\sqrt{\bar{\alpha} y \ln Q^2})$, while the formula for $n^{(1)}$ is rederived below, see Eq. (24).

interpreted as the probability that a dipole of size x_{01} split to two dipoles of sizes x_{02} and x_{12} respectively (up to dx_{02} and dx_{12} resp.) when the rapidity increases by dy .

Finally, it will prove convenient to introduce logarithmic dipole sizes $\rho_{ij} = \ln x_{01}^2/x_{ij}^2$. In this case, the splitting probability reads $\tilde{K}(\rho_{02}, \rho_{12})d\rho_{02}d\rho_{12}dy$, where

$$\tilde{K}(\rho_{02}, \rho_{12}) = \frac{\bar{\alpha}}{\sqrt{\left[(e^{-\rho_{12}/2} + e^{-\rho_{02}/2})^2 - 1\right] \left[1 - (e^{-\rho_{12}/2} - e^{-\rho_{02}/2})^2\right]}}. \quad (5)$$

Note that due to scale invariance, the kernel effectively depends on two independent real variables only.

3.2 Dipole number

Let us introduce the probability $P_n(r_s; x_{01}, y)$ of having n dipoles of size larger than r_s after evolution over the rapidity y , starting with a single dipole of size x_{01} . It is easy to establish an equation for P_n . To this aim, we assume that $P_n(r_s; x_{01}, y)$ is known for all n and all x_{01} and we express $P_n(r_s; x_{01}, y + dy)$, merely translating the branching process described in Sec. 3.1 into an equation:

$$P_n(r_s; x_{01}, y + dy) = P_n(r_s; x_{01}, y) \left(1 - dy \int dx_{02} dx_{12} K(x_{02}, x_{12}; x_{01})\right) + dy \int dx_{02} dx_{12} K(x_{02}, x_{12}; x_{01}) \sum_{m=1}^{n-1} P_m(r_s; x_{02}, y) P_{n-m}(r_s; x_{12}, y). \quad (6)$$

Hence

$$\frac{\partial P_n(r_s; x_{01}, y)}{\partial y} = \int dx_{02} dx_{12} K(x_{02}, x_{12}; x_{01}) \left[\sum_{m=1}^{n-1} P_m(r_s; x_{02}, y) P_{n-m}(r_s; x_{12}, y) - P_n(r_s; x_{01}, y) \right]. \quad (7)$$

This system of equations for the set of P_n 's may be represented by a single equation for the generating function Z of the factorial moments of the dipole number, which is defined as

$$Z(r_s; x_{01}, y|u) = \sum_{n=1}^{\infty} u^n P_n(r_s; x_{01}, y). \quad (8)$$

Indeed, Z is easily seen to obey the Balitsky-Kovchegov (BK) equation⁴ [20, 21]

$$\frac{\partial}{\partial y} Z(r_s; x_{01}, y|u) = \int dx_{02} dx_{12} K(x_{02}, x_{12}; x_{01}) [Z(r_s; x_{02}, y|u) Z(r_s; x_{12}, y|u) - Z(r_s; x_{01}, y|u)]. \quad (9)$$

Since the initial condition is a single dipole of size $x_{01} > r_s$, then obviously

$$Z(r_s; x_{01}, y = 0|u) = u. \quad (10)$$

We also have

$$Z(r_s; x_{01}, y|u = 1) = 1 \quad (11)$$

⁴ Strictly speaking, the BK equation was established as an equation for the S -matrix element for the forward elastic scattering of a dipole off a large nucleus. The evolution of the generating function Z we discuss here was first addressed in Ref. [11]. The two evolution equations can be written in the very same form.

from the unitarity relation $\sum_{n=1}^{\infty} P_n = 1$.

The factorial moments $n^{(k)}$ of the dipole numbers are obtained from Z by derivation with respect to the dummy variable u :

$$n^{(k)}(r_s; x_{01}, y) \equiv \langle n(n-1) \cdots (n-k+1) \rangle = \left. \frac{\partial^k}{\partial u^k} \right|_{u=1} Z(r_s; x_{01}, y|u). \quad (12)$$

Applying k times the derivation operator to the BK equation (9), we see that the set of the factorial moments $n^{(k)}$ solves a hierarchy of integro-differential equations:

$$\begin{aligned} \frac{\partial}{\partial y} n^{(k)}(r_s; x_{01}, y) = \int dx_{02} dx_{12} K(x_{02}, x_{12}; x_{01}) & \left[n^{(k)}(r_s; x_{02}, y) + n^{(k)}(r_s; x_{12}, y) - n^{(k)}(r_s; x_{01}, y) \right. \\ & \left. + \sum_{j=1}^{k-1} \binom{k}{j} n^{(k-j)}(r_s; x_{02}, y) n^{(j)}(r_s; x_{12}, y) \right]. \quad (13) \end{aligned}$$

The equation for $n^{(1)}$ is the dipole version of the usual BFKL equation for the mean gluon number. Taking into account the initial condition $n^{(1)}(r_s; x_{01}, y=0) = \Theta(\ln x_{01}^2/r_s^2)$ (single dipole of size x_{01}), its solution reads⁵

$$n^{(1)}(r_s; x_{01}, y) = \int_{\frac{1}{2}-i\infty}^{\frac{1}{2}+i\infty} \frac{d\gamma}{2i\pi\gamma} e^{\bar{\alpha}\chi(\gamma)y} \left(\frac{x_{01}^2}{r_s^2} \right)^\gamma, \quad (14)$$

where $\chi(\gamma) = 2\psi(1) - \psi(\gamma) - \psi(1-\gamma)$.

The higher moments obey an evolution equation which has the same kernel as the BFKL equation, but with a nontrivial source term represented by the inhomogeneous term in Eq. (13).

3.3 Integral expression for the higher moments

It is useful to introduce the number density $f(x; x_{01}, y)$ of dipoles of transverse size x present in the system after evolution of an initial dipole of size x_{01} over y units of rapidity. We define f in such a way that

$$\int_{r_s^2}^{+\infty} \frac{dx^2}{x^2} f(x; x_{01}, y) = n(r_s; x_{01}, y) \quad (15)$$

is the integrated number of dipoles. The mean dipole number density $f^{(1)} = \langle f \rangle$ reads

$$f^{(1)}(x; x_{01}, y) = \int_{\frac{1}{2}-i\infty}^{\frac{1}{2}+i\infty} \frac{d\gamma}{2i\pi} e^{\bar{\alpha}\chi(\gamma)y} \left(\frac{x_{01}^2}{x^2} \right)^\gamma. \quad (16)$$

We can readily express $n^{(2)}$ with the help of $f^{(1)}$ and $n^{(1)}$. One easily checks⁶ that the following formula holds true:

$$\begin{aligned} n^{(2)}(r_s; x_{01}, y) = 2 \int \frac{dx_{23}^2}{x_{23}^2} \int_0^y dy_1 f^{(1)}(x_{23}; x_{01}, y_1) \\ \times \int dx_{24} dx_{34} K(x_{24}, x_{34}; x_{23}) n^{(1)}(r_s; x_{24}, y-y_1) n^{(1)}(r_s; x_{34}, y-y_1). \quad (17) \end{aligned}$$

⁵Note that with our definition of $n^{(1)}(r_s; x_{01}, y)$, it only depends on the dipole size and not on its orientation nor on the position of its center in the transverse plane. The solution to the BFKL equation we give here is restricted to zero conformal spin.

⁶Take for instance the derivative of Eq. (17) with respect to y and identify its r.h.s. to the r.h.s. of the evolution equation for $n^{(2)}$ in Eq. (13) with $k=2$.

As for the higher moments of n , similar equations may be written to express $n^{(k)}$ with the help of the $n^{(j)}$'s with $j < k$. The existence of such recursion relations is of course just related to the tree structure of the dipole evolution.

4 Collinear limit

Let us first study the collinear limit in which r_s is much smaller than the size x_{01} of the initial dipole. The dominant contribution to the moments of the dipole number is given by the configurations in which successive dipole splittings are strongly ordered in size, namely $x_{02} \ll x_{01}$ and $x_{12} \simeq x_{01}$ or $x_{02} \simeq x_{01}$ and $x_{12} \ll x_{01}$. This translates into inequalities for the logarithmic dipole sizes introduced above in Sec. 3.1, $\rho_{02} > 0$ and $\rho_{12} \simeq 0$ or $\rho_{02} \simeq 0$ and $\rho_{12} > 0$. Technically, the BFKL kernel boils down to a uniform distribution in the logarithm of the dipole sizes: $\tilde{K}(\rho_{02}, \rho_{12}) \simeq \frac{\bar{\alpha}}{2} [\Theta(\rho_{02})\delta(\rho_{12}) + \Theta(\rho_{12})\delta(\rho_{02})]$.

We write $\rho_s = \ln x_{01}^2/r_s^2$ and use logarithmic variables as the argument of Z that represents the dipole sizes. The BK equation (9) simplifies to

$$\partial_y Z(\rho_s, y|u) = \bar{\alpha} Z(\rho_s, y|u) \int_0^{\rho_s} d\rho' [Z(\rho', y|u) - 1]. \quad (18)$$

The upper bound on the ρ' integration implements the fact that a dipole of a given size cannot split to larger dipoles in the collinear limit.

4.1 Moments of the dipole number

In the same manner as in Sec. 3, the equations for the factorial moments $n^{(k)}$ of the dipole number are easily obtained by taking k derivatives of the BK equation in the collinear limit (18) with respect to u , at $u = 1$:

$$\partial_y n^{(k)}(\rho_s, y) - \bar{\alpha} \int_0^{\rho_s} d\rho' n^{(k)}(\rho', y) = \bar{\alpha} \sum_{j=1}^{k-1} \binom{k}{j} n^{(j)}(\rho_s, y) \int_0^{\rho_s} d\rho' n^{(k-j)}(\rho', y), \quad (19)$$

namely

$$\begin{cases} \partial_y n^{(1)}(\rho_s, y) - \bar{\alpha} \int_0^{\rho_s} d\rho' n^{(1)}(\rho', y) = 0, \\ \partial_y n^{(2)}(\rho_s, y) - \bar{\alpha} \int_0^{\rho_s} d\rho' n^{(2)}(\rho', y) = 2\bar{\alpha} n^{(1)}(\rho_s, y) \int_0^{\rho_s} d\rho' n^{(1)}(\rho', y) \\ \dots \end{cases} \quad (20)$$

For the purpose of trying to understand the properties of the solutions to the hierarchy (19), it is convenient to start over with Eq. (18) and to rewrite it as a second-order partial differential equation

$$\partial_{\rho_s} \partial_y \ln Z(\rho_s, y|u) = \bar{\alpha} [Z(\rho_s, y|u) - 1]. \quad (21)$$

The left-hand side is a second derivative of the generating function of the factorial cumulants $n_c^{(k)}$ of the dipole multiplicity, connected to the factorial moments $n^{(k)}$ through the relations

$$n_c^{(1)} = n^{(1)}, \quad n_c^{(2)} = n^{(2)} - [n^{(1)}]^2, \quad n_c^{(3)} = n^{(3)} - 3n^{(2)}n^{(1)} + 2[n^{(1)}]^3, \dots \quad (22)$$

Introducing further the variables $z = 2\sqrt{\bar{\alpha} y \rho_s}$ and $\tilde{z} = \frac{1}{2}\sqrt{\rho_s/\bar{\alpha} y}$, the differential operator becomes $\partial_{\rho_s} \partial_y = \bar{\alpha} \left(\partial_z^2 + \frac{1}{z} \partial_z - \frac{\tilde{z}^2}{z^2} \partial_{\tilde{z}}^2 - \frac{\tilde{z}}{z^2} \partial_{\tilde{z}} \right)$. We then see that it is consistent to look for

solutions which are independent of the variable \tilde{z} : We will focus on such solutions in what follows. To obtain the differential equations in terms of the z variable, it is convenient to start from Eq. (21) and take again k derivatives with respect to u

$$\begin{cases} (z^2 \partial_z^2 + z \partial_z - z^2) n_c^{(1)}(z) = 0, \\ (z^2 \partial_z^2 + z \partial_z - z^2) n_c^{(2)}(z) = z^2 [n^{(1)}(z)]^2, \\ (z^2 \partial_z^2 + z \partial_z - z^2) n_c^{(3)}(z) = z^2 \left\{ 3n^{(2)}(z)n^{(1)}(z) - 2[n^{(1)}(z)]^2 \right\}, \\ \dots \end{cases} \quad (23)$$

We note that the operator appearing in the homogeneous part of these equations is the kernel of a Bessel equation. The solution to the hierarchy cannot be expressed fully analytically, however, the large- z asymptotics are simple and partially known. Indeed, the same kind of equations appear in the context of jet physics [22, 23]. Let us nevertheless discuss these asymptotics in some detail.

The solution of the equation for the first cumulant (or moment) $n_c^{(1)} = n^{(1)}$ with the initial condition $n^{(1)}(\rho_s, y=0) = 1$ is a modified Bessel function of the first kind:

$$n^{(1)}(z) = I_0(z). \quad (24)$$

The first moment $n^{(1)}$ is the mean dipole number. Another notation for $n^{(1)}$ that we shall use in what follows is \bar{n} .

The next equations in the hierarchy are seen to exhibit the same kernel as the equation for $n^{(1)}$: Only the inhomogeneous term differs. As for $n_c^{(2)}$, we find an exact expression which, once re-expressed in terms of moments through Eq. (22), reads

$$n^{(2)}(z) = I_0^2(z) + I_0(z) \int_0^z dz' z' K_0(z') I_0^2(z') - K_0(z) \int_0^z dz' z' I_0^3(z'). \quad (25)$$

The above integrals do not have a simpler expression, however, we may obtain the large- z expansion of $n^{(2)}$ from the expansion of the Bessel functions:

$$I_0(z) \underset{z \rightarrow \infty}{=} \frac{e^z}{\sqrt{2\pi z}} \left(1 + \frac{1}{8z} + \dots \right), \quad K_0(z) \underset{z \rightarrow \infty}{=} \sqrt{\frac{\pi}{2z}} e^{-z} \left(1 - \frac{1}{8z} + \dots \right) \quad (26)$$

To first order in $1/z$ and switching back to the (ρ_s, y) variables, we get

$$\frac{n^{(2)}(\rho_s, y)}{[n^{(1)}(\rho_s, y)]^2} = \frac{4}{3} \left(1 + \frac{1}{12\sqrt{\bar{\alpha} y \rho_s}} + O(1/\bar{\alpha} y \rho_s) \right). \quad (27)$$

We may repeat this procedure for the higher moments. For example we find for $n^{(3)}$:

$$\frac{n^{(3)}(\rho_s, y)}{[n^{(1)}(\rho_s, y)]^3} = \frac{9}{4} \left(1 + \frac{5}{12\sqrt{\bar{\alpha} y \rho_s}} + O(1/\bar{\alpha} y \rho_s) \right) \quad (28)$$

The generic structure is

$$\frac{n^{(k)}(\rho_s, y)}{[n^{(1)}(\rho_s, y)]^k} = C_k + O(1/\sqrt{\bar{\alpha} y \rho_s}), \quad (29)$$

where the coefficients C_k are constants.

The coefficients C_k may be computed by inserting the *Ansatz* $n^{(k)}(z) = C_k [\bar{n}(z)]^k$ into the hierarchy (19), and by recalling that $n^{(1)}(\rho_s, y) \simeq e^{2\sqrt{\alpha}\rho_s y}$. The C_k are then seen to obey the following recursion [22]:

$$C_{k \geq 2} = \frac{k}{k^2 - 1} \sum_{j=1}^{k-1} \binom{k}{j} \frac{C_j C_{k-j}}{k-j}, \quad C_1 = 1. \quad (30)$$

For large k , C_k converges⁷ fastly to $C_k \simeq 2k k! (c_{\text{DL}})^k$, where $c_{\text{DL}} = 0.391 \dots$.

4.2 Multiplicity distribution

From the knowledge of the large- k and large- z asymptotics of the factorial moments (and hence of the ordinary moments, due to the exponential increase of $n^{(k)}(z)$ at large z), one can infer the large- n behavior of the distribution of the dipole multiplicity n . Indeed,

$$n^{(k)}(z) = \sum_{n=1}^{\infty} n^k P_n(z) \simeq \int_0^{+\infty} dn n^k P_n(z) \quad (31)$$

where the second approximate equality holds for large k , since the sum over n is dominated by large values of n in that limit.

We continue analytically the moment index k to complex values, and invert this equation as

$$P_n(z) = \int \frac{dk}{2i\pi} n^{-k-1} n^{(k)}(z) \quad (32)$$

which when we specialize to the collinear limit reads

$$P_n^{\text{DL}}(z) = \frac{2}{c_{\text{DL}} \bar{n}_{\text{DL}}(z)} \int \frac{dk}{2i\pi} k \Gamma(k+1) \left(\frac{c_{\text{DL}} \bar{n}_{\text{DL}}(z)}{n} \right)^{k+1}. \quad (33)$$

A straightforward calculation leads to the final result

$$P_n^{\text{DL}} \propto \frac{2}{c_{\text{DL}} \bar{n}_{\text{DL}}} \left(\frac{1}{c_{\text{DL}}} \frac{n}{\bar{n}_{\text{DL}}} - 1 \right) \exp \left(-\frac{1}{c_{\text{DL}}} \frac{n}{\bar{n}_{\text{DL}}} \right). \quad (34)$$

Note that the probability distribution P_n^{DL} exhibits Koba-Nielsen-Olesen (KNO) scaling [24], namely $\bar{n}_{\text{DL}} P_n^{\text{DL}}$ is a function of n/\bar{n}_{DL} only.

One may think that the qualitative properties of this distribution would be kept when one gives up the strong ordering of the transverse momenta. This is actually not at all the case, as we will demonstrate in the next section.

5 Full BFKL evolution

When the ordering condition between r_s and x_{01} is released, then the full BK equation has to be solved. The difference between the full BK equation (9) and its DL approximation (18) is that the former allows splittings to larger dipoles, while the latter describes only splittings to

⁷ It is straightforward to check this asymptotic form for the solution by inserting it into Eq. (30). The value of the constant c_{DL} is obtained numerically.

smaller dipoles.

We shall now review the asymptotics of the solution, which were first derived in Ref. [25], and interpret them. The most convenient is to analyze the equations for the moments. Let us start by discussing the second-order factorial moment $n^{(2)}$.

5.1 Second-order moment

The second-order factorial moment is obtained by inserting the expressions of the first moments (14),(16) into Eq. (17). Using the logarithmic variables $\rho_s = \ln x_{01}^2/r_s^2$ and $\rho_1 = \ln x_{01}^2/x_{23}^2$, $n^{(2)}$ can be cast as

$$n^{(2)}(\rho_s, y) = 2 \int_{-\infty}^{+\infty} d\rho_1 \int_0^y dy_1 \int \frac{d\gamma}{2i\pi} \frac{d\gamma_1}{2i\pi\gamma_1} \frac{d\gamma_2}{2i\pi\gamma_2} P_3(\gamma_1, \gamma_2) e^{\mathcal{E}_2(\gamma, \gamma_1, \gamma_2, y_1, \rho_1; \rho_s, y)}, \quad (35)$$

where

$$\mathcal{E}_2 = \bar{\alpha} y_1 \chi(\gamma) + \gamma \rho_1 + \bar{\alpha}(y - y_1)[\chi(\gamma_1) + \chi(\gamma_2)] + (\gamma_1 + \gamma_2)(\rho_s - \rho_1) \quad (36)$$

and

$$P_3(\gamma_1, \gamma_2) = \int d\delta_1 d\delta_2 \tilde{K}(\delta_1, \delta_2) e^{-\gamma_1 \delta_1 - \gamma_2 \delta_2} \quad (37)$$

($\delta_1 = \ln x_{23}^2/x_{24}^2$ and $\delta_2 = \ln x_{23}^2/x_{34}^2$). We want to evaluate $n^{(2)}$ in the limit of large ρ_s and large y .

We start by looking for a saddle point in the γ , γ_1 and γ_2 variables independently, ρ_1 and y_1 being fixed for the time being. We require that the partial derivative of \mathcal{E}_2 with respect to these variables vanish, which leads to the unique solution

$$\chi'(\gamma_c^{(2)}) = -\frac{\rho_1}{\bar{\alpha} y_1}, \quad \chi'(\gamma_{1c}^{(2)}) = -\frac{\rho_s - \rho_1}{\bar{\alpha}(y - y_1)} \quad \text{and} \quad \gamma_{2c}^{(2)} = \gamma_{1c}^{(2)}. \quad (38)$$

Performing this integral by the steepest-descent method, the pair multiplicity reads

$$n^{(2)}(\rho_s, y) \simeq \frac{2}{(2\pi)^{3/2}} \int_{-\infty}^{+\infty} d\rho_1 \int_0^y dy_1 \frac{P_3(\gamma_{1c}^{(2)}, \gamma_{2c}^{(2)})}{\gamma_{1c}^{(2)} \gamma_{2c}^{(2)}} \times \frac{1}{\sqrt{|\det H|}} e^{\mathcal{E}_2(\gamma_c^{(2)}, \gamma_{1c}^{(2)}, \gamma_{2c}^{(2)}, y_1, \rho_1; \rho_s, y)}, \quad (39)$$

where H is the matrix of the second derivatives of \mathcal{E}_2 evaluated at the saddle point.

The saddle point $(\gamma_c^{(2)}, \gamma_{1c}^{(2)} = \gamma_{2c}^{(2)})$ depends on y_1 and on ρ_1 , over which we still need to integrate. We are going to search for a stationary point of \mathcal{E}_2 in the two remaining integration variables y_1 and ρ_1 . The partial derivatives of \mathcal{E}_2 with respect to ρ_1 and y_1 taken at the saddle point read

$$\frac{\partial \mathcal{E}_2}{\partial \rho_1} = \gamma_c^{(2)} - 2\gamma_{1c}^{(2)} \quad (40a)$$

$$\frac{\partial \mathcal{E}_2}{\partial y_1} = \bar{\alpha} [\chi(\gamma_c^{(2)}) - 2\chi(\gamma_{1c}^{(2)})]. \quad (40b)$$

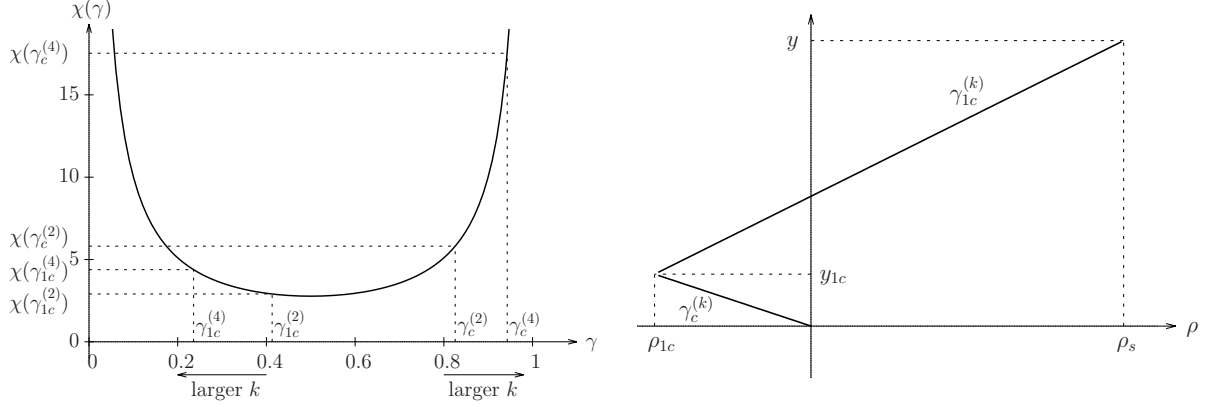


Figure 2: *Left*: Characteristic function of the BFKL kernel and the global saddle point solutions for the second and the fourth moments. One sees that the higher the moment index, the more the anomalous dimensions corresponding to the first and the second steps of the evolution get attracted by the collinear and anticollinear singularities at $\gamma = 1$ and $\gamma = 0$ respectively. *Right*: Schematic representation of the evolution path selected by the moments $n^{(k)}$ in the (ρ, y) plane.

5.1.1 Global saddle point

For a global saddle point of the multiple integral to exist, the derivatives in Eq. (40) must vanish simultaneously, which requires

$$\gamma_{1c}^{(2)} = \gamma_{2c}^{(2)} = \frac{\gamma_c^{(2)}}{2}, \quad \chi(\gamma_c^{(2)}) = 2\chi(\gamma_{1c}^{(2)}). \quad (41)$$

Eq. (41) can be solved numerically: $\gamma_{1c}^{(2)} = 0.412796 \dots$. The solution is represented in Fig. 2. We note that $\chi'(\gamma_{1c}^{(2)}) < 0$ and $\chi'(\gamma_c^{(2)}) > 0$. Once the value of $\gamma_{1c}^{(2)}$ is fixed, Eq. (38) implies

$$\bar{\alpha}y_{1c} = \frac{\chi'(\gamma_{1c}^{(2)})\bar{\alpha}y + \rho_s}{\chi'(\gamma_{1c}^{(2)}) - \chi'(\gamma_c^{(2)})}, \quad \rho_{1c} = -\chi'(\gamma_c^{(2)})\bar{\alpha}y_{1c}. \quad (42)$$

We note that this solution requires ρ_{1c} to be negative. Conversely, if $\rho_{1c} < 0$, then this saddle point solution exists provided $0 < y_{1c} < y$, a condition that is satisfied whenever the external parameters obey the ordering relation

$$\rho_s < -\chi'(\gamma_{1c}^{(2)})\bar{\alpha}y, \quad (43)$$

which follows from the first equation in (42), conveniently rewritten as

$$\rho_s = -\chi'(\gamma_{1c}^{(2)})\bar{\alpha}y + \bar{\alpha}y_{1c} [\chi'(\gamma_{1c}^{(2)}) - \chi'(\gamma_c^{(2)})] \quad (44)$$

and from the negativity of the second term in the r.h.s.

The physical picture of this solution is the following: Starting from the dipole of size x_{01} , the first part of the evolution, which typically takes place over the first $\bar{\alpha}y_{1c}$ units of rapidity, produces a larger dipole (since ρ_{1c} is negative). The latter decays to two dipoles, which subsequently evolve independently over the rapidity range $y - y_{1c}$. The saddle-point solution is represented on the graph of the χ -function in Fig. 2, together with the evolution path in the (ρ, y) plane.

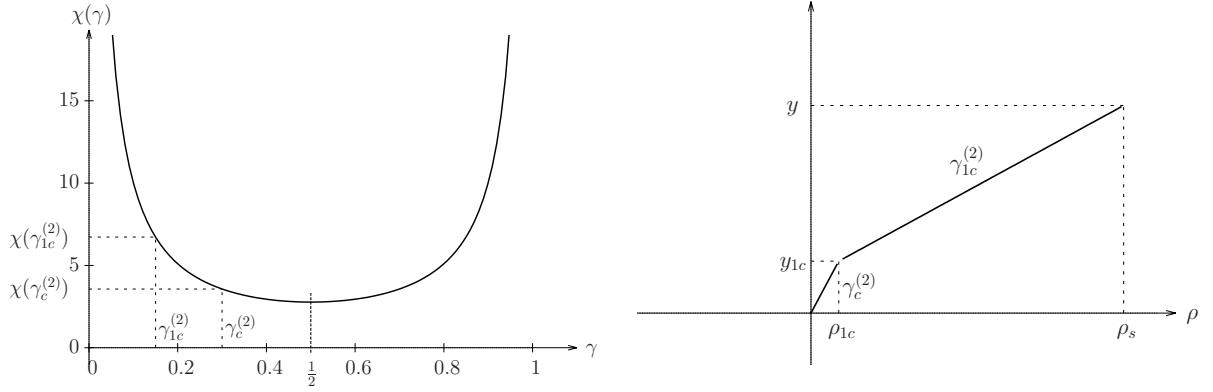


Figure 3: *Left*: Solution for the second moment in the case in which there is no global saddle point. $\gamma_c^{(2)}$ and $\gamma_{1c}^{(2)}$ are not completely fixed in this case: They however satisfy the relation $2\gamma_{1c}^{(2)} = \gamma_c^{(2)} < \frac{1}{2}$. *Right*: Schematic representation of the evolution path selected by the moment $n^{(2)}$ in the (ρ, y) plane. There is no step backward. This kind of path is favored when $\bar{\alpha}y$ is not large compared to ρ_s .

5.1.2 Connection with the DL limit

If the global saddle-point solution does not exist, then the values of ρ_1 that contribute to the integration in Eq. (35) are essentially positive. In this case, the saddle point equations (38) impose that both $\gamma_{1c}^{(2)}$ and $\gamma_c^{(2)}$ be less than $\frac{1}{2}$. We can require again the stationarity of \mathcal{E}_2 with respect to the variations of ρ , which, using (40a), leads to the condition $\gamma_c^{(2)} = 2\gamma_{1c}^{(2)}$. Hence $2\gamma_{1c}^{(2)} = \gamma_c^{(2)} < \frac{1}{2}$, which trivially implies $\chi(\gamma_c^{(2)}) < 2\chi(\gamma_{1c}^{(2)})$. Then, according to Eq. (40b) the integral is strongly dominated by the region $y_1 \ll y$. Indeed, an upper bound for the values of $\bar{\alpha}y_1$ which contribute significantly to the integral is⁸ $1/[2\chi(\frac{1}{4}) - \chi(\frac{1}{2})] = 0.18 \dots$, a number which is small compared to $\bar{\alpha}y$.

Note that $\chi'(\gamma_c^{(2)}) > \chi'(\gamma_{1c}^{(2)})$: From the saddle-point equation (38), we see that the relevant integration region for ρ_1 is $0 < \rho_1 < \rho_s y_1/y \ll \rho_s$. Hence the evolution that leads to a pair of dipoles just consists in two independent evolutions of single dipoles starting almost right from the beginning of the branching process. In this regime, the collinear limit studied in Sec. 4 is relevant throughout the whole evolution. The solution in this case is represented in Fig. 3.

The solutions we have just found are qualitatively different from what one would find in the case of a branching-diffusion process. This question is addressed in some detail in Appendix A. The dipole model can be identified with such a process when one observes the dipole density at a fixed impact parameter, but when one integrates over the impact parameter as we do here, then the hotspots generated by the collinear singularities dominate, and the dipole branching is no longer a diffusion in the logarithmic dipole sizes.

We are now going to investigate in the same spirit the higher moments of the dipole multiplicity.

⁸ This bound may be derived from the form of the y -dependence of \mathcal{E}_2 (see Eq. (40b)) and from the convexity properties of the function $2\chi(\gamma) - \chi(2\gamma)$.

5.2 Higher moments

The integral expression of the moment of order k is a complicated multiple integral of products of mean dipole numbers and densities. For its complexity, we will not be able to study in detail its limits in the same way as for $n^{(2)}$. Therefore, we will assume that the global saddle-point solution essentially consists in two steps. We will see that for large enough values of k , the global saddle point always exists. The first step is then the production of a larger dipole and the second its decay into much smaller dipoles.

Let us write directly the saddle-point solution:

$$n^{(k)}(\rho_s, y) \propto e^{\mathcal{E}_k(\gamma_c^{(k)}, \gamma_{1c}^{(k)}, \dots, \gamma_{kc}^{(k)}; y_{1c}, \rho_{1c}; \rho_s, y)}, \quad (45)$$

where

$$\mathcal{E}_k = \bar{\alpha} y_{1c} \chi(\gamma_c^{(k)}) + \gamma_c^{(k)} \rho_{1c} + \bar{\alpha}(y - y_{1c}) \left[\chi(\gamma_{1c}^{(k)}) + \dots + \chi(\gamma_{kc}^{(k)}) \right] + (\gamma_{1c}^{(k)} + \dots + \gamma_{kc}^{(k)})(\rho_s - \rho_{1c}) \quad (46)$$

generalizes Eq. (36) taken at the saddle point, and the following relations must hold true:

$$\gamma_{1c}^{(k)} = \dots = \gamma_{kc}^{(k)} = \frac{\gamma_c^{(k)}}{k}, \quad \chi(\gamma_c^{(k)}) = k \chi(\gamma_{1c}^{(k)}), \quad \chi'(\gamma_c^{(k)}) = -\frac{\rho_1}{\bar{\alpha} y_1}, \quad \chi'(\gamma_{1c}^{(k)}) = -\frac{\rho_s - \rho_1}{\bar{\alpha}(y - y_1)}. \quad (47)$$

For large k , according to the first relation, necessarily $\gamma_{1c}^{(k)} \rightarrow 0$. The second relation imposes $\gamma_c^{(k)} \rightarrow 1$. Hence one may replace the complete expression of $\chi(\gamma)$ by its collinear $\chi(\gamma) \simeq 1/\gamma$ (resp. anticollinear $\chi(\gamma) \simeq 1/(1-\gamma)$) limit whenever this function or its derivative are evaluated at $\gamma = \gamma_{1c}^{(k)}$ (resp. $\gamma = \gamma_c^{(k)}$). The saddle-point equations lead to $\gamma_c^{(k)} \simeq 1 - 1/k^2$, $\gamma_{1c}^{(k)} \simeq 1/k$ at large k . Then

$$\bar{\alpha} y_{1c} \simeq \bar{\alpha} y / k^2 \quad \text{and} \quad \rho_{1c} \simeq -k^2 \bar{\alpha} y. \quad (48)$$

The saddle-point solution should exist as soon as $k > \sqrt{\rho_s / \bar{\alpha} y}$: Hence for large enough k , it will always be the only relevant solution.

Using this determination of the saddle-point parameters, we find $\mathcal{E}_k \simeq \rho_s + k^2 \bar{\alpha} y$. Hence the large- k expression for the k -th moment of the dipole number is

$$n^{(k)}(\rho_s, y) \propto e^{\rho_s + k^2 \bar{\alpha} y}. \quad (49)$$

The interpretation of this solution is straightforward. The k dipoles that are measured at rapidity y stem from the evolution of a “common ancestor”, which was produced at rapidity $y_{1c} \simeq y/k^2 \rightarrow 0$ (at large k). This ancestor dipole has a size which is of the order of $e^{k^2 \bar{\alpha} y}$ times bigger than the initial dipole.

We have actually just recovered the picture that was argued for in Ref. [25], where the backward step of the evolution was assumed to coincide with the very first splitting, and the further evolution was replaced by its collinear limit.

5.3 Multiplicity distribution and physical picture

From the expression of the moments of the dipole multiplicity of order k in the large- k limit, we can go back to the distribution using the relation (32) and replacing therein $n^{(k)}$ by the

expression in Eq. (49). The integral to perform is Gaussian. The result reads [25]

$$P_n(r_s; x_{01}, y) \propto \frac{x_{01}^2}{r_s^2} \frac{1}{n} \exp\left(-\frac{\ln^2 n}{4\bar{\alpha}y}\right). \quad (50)$$

The large- n tail of this distribution is much fatter than the one of the DL limit (34). Moreover, this probability distribution does not obey KNO scaling.

If one focusses on larger multiplicities, then the evolution goes through large-size dipoles, much larger than the initial dipole. If the latter models a hadron of typical size $1/\Lambda_{\text{QCD}}$, the production of much larger dipoles should be cut off by confinement. We shall now introduce a qualitative model for these effects, and propose a solution.

6 Evolution in the presence of confinement

Confinement is expected to act as a cutoff that prevents dipoles of size larger than typically $R \sim 1/\Lambda_{\text{QCD}}$ to be created. Here we are going to pick a simple model that enable us to arrive at analytical results.

To this aim, we go back to the equation (13) for the moments of the dipole number and implement a Gaussian cutoff on the size of the produced dipoles. For technical reasons, it is convenient to use the form of the kernel in Eq. (3) and to enforce the cutoff through the substitution

$$K_0(\mathbf{x}_2; \mathbf{x}_0, \mathbf{x}_1) \rightarrow \frac{\bar{\alpha}}{2\pi} \frac{x_{01}^2}{x_{02}^2 x_{12}^2} e^{-(x_{02}^2 + x_{12}^2)/(2R^2)} \quad (51)$$

in such a way that Eq. (13) be replaced by

$$\begin{aligned} \frac{\partial}{\partial y} n^{(k)}(r_s; x_{01}, y) = & \bar{\alpha} \int \frac{d^2 \mathbf{x}_2}{2\pi} \frac{x_{01}^2}{x_{02}^2 x_{12}^2} e^{-(x_{02}^2 + x_{12}^2)/(2R^2)} \left[n^{(k)}(r_s; x_{02}, y) + n^{(k)}(r_s; x_{12}, y) \right. \\ & \left. - n^{(k)}(r_s; x_{01}, y) + \sum_{j=1}^{k-1} \binom{k}{j} n^{(k-j)}(r_s; x_{02}, y) n^{(j)}(r_s; x_{12}, y) \right]. \end{aligned} \quad (52)$$

With respect to the case without cutoff studied in the previous section, only dipoles of size less than R may be created with high probability. Hence the larger span for the rapidity evolution is between the dipole sizes R and r_s . It is then natural to try an *Ansatz* of the form

$$n^{(k)}(r_s; x_{01}, y) = \frac{x_{01}^2}{R^2} e^{-x_{01}^2/(2R^2)} C_k \left[n^{(1)}(r_s; R, y) \right]^k \quad (53)$$

for large k . We are going to check that this form is indeed an asymptotic solution.

As in the case of $n^{(1)}$, we may assume that the integral in Eq. (14) is dominated by the value of the integrand at the saddle point γ_s . Discarding the prefactors, we write

$$n^{(1)}(r_s; R, y) \sim \left(\frac{R^2}{r_s^2} \right)^{\gamma_s} e^{\bar{\alpha} y \chi(\gamma_s)} \quad (54)$$

and γ_s solves $\bar{\alpha} y \chi'(\gamma_s) + \ln R^2/r_s^2 = 0$. Looking at Eq. (52), we see that the nonlinear terms dominate the large- y solution because of the y -dependence of our *Ansatz* for $n^{(k)}$. Inserting the

latter into Eq. (52) deprived of the linear terms in the right-hand side, the integro-differential equation for $n^{(k)}$ becomes a recursion for the constants C_k

$$e^{-x_{01}^2/(2R^2)} k C_k = \frac{1}{\chi(\gamma_s)} \sum_{j=1}^{k-1} \binom{k}{j} \int \frac{d^2 \mathbf{x}_2}{2\pi R^2} e^{-(x_{02}^2 + x_{12}^2)/R^2} C_j C_{k-j} \quad (55)$$

which is easily simplified to

$$C_k = \frac{1}{4\chi(\gamma_s)} \frac{1}{k} \sum_{j=1}^{k-1} \binom{k}{j} C_j C_{k-j}. \quad (56)$$

For large k , this recursion is solved by $C_k \simeq 4\chi(\gamma_s) k! c^k$, where the constant c depends on C_0 on which we have no control since the linear term we dropped in the equation (52) for the moments plays a central role for the moments of low k .

From the large- k moments, one can infer the large- n behavior of the probability distribution. We find

$$P_n(r_s; x_{01}, y) \propto 4\chi(\gamma_s) \frac{x_{01}^2}{R^2} e^{-x_{01}^2/(2R^2)} \frac{1}{c\bar{n}} e^{-n/(c\bar{n})}. \quad (57)$$

Note that the value of the constant c depends on the form of the recursion (56), which in turn may depend on the details of the infrared cutoff. Therefore we do not expect this constant to be universal. However, the exponential form⁹ is very likely to be universal, because it requires no more than the existence of an infrared absorptive boundary in the evolution. Numerical checks would be useful in order to confirm the solution in Eq. (57) and to probe its universality.

7 Summary and outlook

In this paper, we studied the distribution of the multiplicity of the particles produced in high-energy onium-nucleus collisions in the forward rapidity region of the onium, as the simplest possible model for proton-nucleus collisions.

We investigated different kinematical regimes. First, we observed that in the large-rapidity and small-size regime in which the double-logarithmic (DL) approximation makes sense, the problem formally maps to jet evolution. We then showed that when the DL approximation is released, the large-multiplicity distribution becomes much fatter, due to the production of very large dipoles in the course of the evolution. However, confinement does not allow for such evolution paths: Once the latter are cut off, the tail of the multiplicity distribution becomes a decreasing exponential. The analytical results we obtained in the different regimes of the dipole evolution are shown in Fig. 4 and compared to Monte Carlo simulations of a simple one-dimensional toy model described in Appendix B.

A natural extension of this work would be to try and build a more realistic model for proton-nucleus collisions beyond the dipole model, in order to allow for sensible comparisons with LHC experimental data. From a more theoretical perspective, if our assumption on the relation between event-by-event partonic fluctuations in the initial state and final-state multiplicity fluctuations is correct, then the tails of the multiplicity distribution stem from dense states of gluons present in the wavefunction of the initially dilute projectile (the onium, or the proton). Understanding these rare events may open a new window on very high-density quantum states.

⁹A decreasing exponential is also the dominant behavior of the tail of the negative binomial distribution found in the glasma model, see Refs. [26, 27].

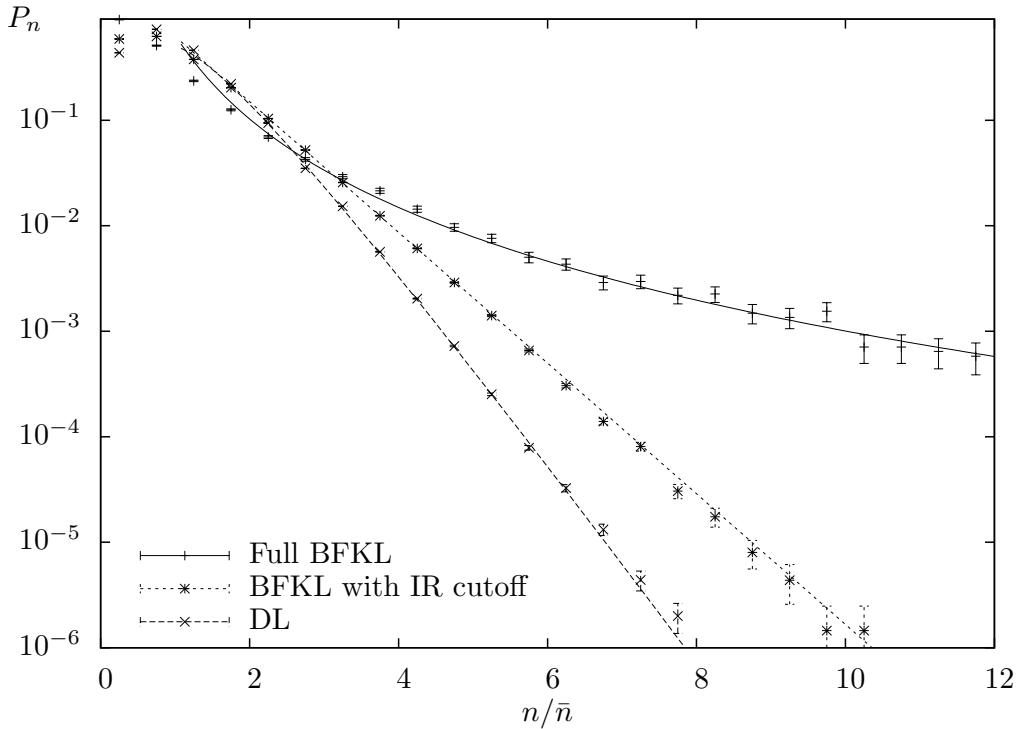


Figure 4: Distribution of the fluctuations of the multiplicity around its expected value \bar{n} from a Monte Carlo simulation of a simplified model (see Appendix B). The lines represent fits of the analytical formulas (50), (57) and (34) (from top to bottom).

Acknowledgments

We acknowledge support from the France-US binational exchange program PICS, project title: “Fundamental properties of quantum chromodynamics at high energy and high density and applications at the LHC”. T.L. benefited from a Doctoral Mobility Grant awarded by the Direction des Relations Internationales of École Polytechnique at the time when this project was initiated. A.H.M. acknowledges support from the Office of Science of the U.S. Department of Energy, Grant No. DE-FG02-92ER40699. We thank Dr. Cyrille Marquet for suggesting references.

A Dipole pair multiplicity in a branching-diffusion model

In this appendix, we shall assume that $\chi(\gamma)$ is a second-order polynomial:

$$\chi(\gamma) = \chi_0 + (\gamma - \gamma_0)\chi'_0 + \frac{1}{2}(\gamma - \gamma_0)^2\chi''_0, \quad (58)$$

where $0 < \gamma_0 < 1$ and χ_0 , χ'_0 , and $\chi''_0 > 0$ are constants. We assume that $\chi(\gamma) > 0$ for all γ . Such a second-order polynomial in γ represents the eigenvalues of a branching-diffusion kernel with a drift. The technical advantage of such a diffusive model is that the integrations over the sizes being Gaussian, they can be performed exactly.

If $\gamma_0 = 0$, $\chi_0 = 1$, $\chi'_0 = 0$ and $\chi''_0 = 2$, this is plain branching Brownian motion. (For a detailed numerical and analytical study of the pair multiplicity in the branching Brownian motion, see Ref. [28]). If instead the constants χ_0 , χ'_0 and χ''_0 coincide with the values of the

functions χ , χ' and χ'' respectively evaluated at γ_0 , with $0 < \gamma_0 < 1$, then Eq. (58) defines the so-called diffusive approximation to the BFKL kernel, which has been studied in QCD. The associated stochastic process is a branching random walk with a drift.

The diffusive approximation to dipole branching would be relevant if one were interested in studying the dipole pair number at a given impact parameter instead of integrating over all impact parameters, as we do in this paper since the observable we consider here requires it. Physically, if the dipole branching process is diffusive, then the excursions through very large dipole sizes during evolution are highly improbable.

Let us rewrite the function $\chi(\gamma)$ in the convenient form $\chi(\gamma) = \lambda - \mu\gamma + \frac{\chi_0''}{2}\gamma^2$, where

$$\lambda = \chi_0 - \gamma_0\chi_0' + \frac{1}{2}\gamma_0^2\chi_0'', \quad \mu = \gamma_0\chi_0'' - \chi_0'. \quad (59)$$

With such a kernel, the mean unintegrated dipole density is a Gaussian in logarithmic dipole sizes

$$f^{(1)}(x; x_{01}, y) = \frac{1}{\sqrt{2\pi\chi_0''\bar{\alpha}y}} \exp \left\{ \lambda\bar{\alpha}y - \frac{\delta\rho^2}{2\chi_0''\bar{\alpha}y} \right\} \quad (60)$$

where we introduced

$$\delta\rho = \rho - \mu\bar{\alpha}y, \quad \rho = \ln \frac{x_{01}^2}{x^2}. \quad (61)$$

This formula shows very clearly that viewed from the lines of constant $\delta\rho$, our process is a branching diffusion with branching rate λ (per unit $\bar{\alpha}y$) and diffusion coefficient $\chi_0''/2$. At variance with BFKL, the branching and the diffusion decouple completely in this class of models.

The mean density of pairs of dipoles of equal size x reads

$$f^{(2)}(x_{01}, x; y) = \langle : [f(x_{01}, x; y)]^2 : \rangle = 2 \int_0^y \lambda\bar{\alpha} dy_1 \int_{-\infty}^{+\infty} d\rho_1 f^{(1)}(\rho_1; y_1) \left[f^{(1)}(\rho - \rho_1; y - y_1) \right]^2. \quad (62)$$

The ρ_1 integration is just a Gaussian integration. We are left with

$$f^{(2)}(x; x_{01}, y) = \frac{\lambda}{\pi\chi_0''y} \int_0^y \frac{dy_1}{\sqrt{1 - y_1^2/y^2}} \exp \left\{ \lambda\bar{\alpha}(2y - y_1) - \frac{\delta\rho^2}{\chi_0''\bar{\alpha}(y + y_1)} \right\}. \quad (63)$$

We are going to study the large- y limit of $f^{(2)}$. There are two interesting cases defined by the relative values of $|\delta\rho|$ and $\chi_0''\bar{\alpha}y$.

Whenever $|\delta\rho|$ is much smaller than $\bar{\alpha}y$, the integral over y_1 is dominated by a region near its lower bound. Indeed, we observe that we can write

$$f^{(2)} = 2 \left[f^{(1)} \right]^2 \int_0^{\lambda\bar{\alpha}y} \frac{d\bar{y}_1}{\sqrt{1 - \bar{y}_1^2/(\lambda\bar{\alpha}y)^2}} \exp \left\{ -\bar{y}_1 \left[1 - \frac{1}{\lambda\chi_0''} \left(\frac{\delta\rho}{\bar{\alpha}y} \right)^2 \frac{1}{1 + \bar{y}_1/(\lambda\bar{\alpha}y)} \right] \right\} \quad (64)$$

The argument of the exponential is negative when $|\delta\rho| < \sqrt{\lambda\chi_0''\bar{\alpha}y}$. The fixed- $\delta\rho$ and large- y expansion of $f^{(2)}$ reads

$$f^{(2)} = 2 \left[f^{(1)} \right]^2 \left[1 + \frac{1}{\lambda\chi_0''} \left(\frac{\delta\rho}{\bar{\alpha}y} \right)^2 + O(1/(\bar{\alpha}y)^2) \right] \xrightarrow{\bar{\alpha}y \gg |\delta\rho|} 2 \left[f^{(1)} \right]^2 \quad (65)$$

In this regime, the “common ancestor” of the pair of dipoles lives at the very beginning of the rapidity evolution, typically within $1/\lambda$ units of $\bar{\alpha}y$ from the start. The picture is similar to

BFKL either in the DL approximation, or with a cutoff modeling confinement.

In the opposite regime, that is when $\delta\rho \gg \bar{\alpha}y$, we write

$$f^{(2)} = 2f^{(1)} \times \lambda \sqrt{\frac{\bar{\alpha}y}{2\pi\chi_0''}} \int_0^y \frac{d\tilde{y}_1}{\sqrt{\tilde{y}_1(2y-\tilde{y}_1)}} \exp \left\{ -\tilde{y}_1 \left[\frac{\delta\rho^2}{4\chi_0''\bar{\alpha}} \frac{1}{y(y-\tilde{y}_1/2)} - \lambda\bar{\alpha} \right] \right\}, \quad (66)$$

where we defined $\tilde{y}_1 = y - y_1$. Thus

$$f^{(2)} \xrightarrow{\bar{\alpha}y \ll |\delta\rho|} 2f^{(1)} \times \lambda \frac{\bar{\alpha}y}{\delta\rho}. \quad (67)$$

In this regime, since the low- \tilde{y}_1 region (i.e. in terms of the initial integration variable, $y_1 \sim y$) dominates the integral in Eq. (66), the evolution is essentially a single path until the very last splittings.

We see that there is no regime in which a large object can be produced at the beginning of the evolution, unlike in the plain BFKL case. This is due to the lack of singularities in the branching-diffusion kernel. Therefore, the diffusive approximation lacks some fundamental features of the BFKL evolution, and should be used with great care when one is interested in the integrated gluon density.¹⁰

B Numerical simulations in a simplified model

In order to test qualitatively the analytical results obtained in this paper, we perform a Monte Carlo simulation of a model that has the main features of the color dipole model, but that is simpler and more manageable numerically.

The model we consider is a simplified version of the color dipole model. The transverse space has only one dimension, and the evolution kernel is reduced to the collinear and anticollinear logarithmic singularities.

Let us introduce the logarithmic variable¹¹ $\rho = \ln x_{01}/r$ to characterize a dipole of generic size r . The equivalent BFKL kernel, that is the rate of splitting of a dipole of (log)size ρ to a dipole of (log)size ρ' , reads

$$d\rho' \frac{dp}{dy}(\rho \rightarrow \rho') = d\rho' \bar{\alpha} \left[\theta(\rho - \rho') + \theta(\rho' - \rho) e^{-(\rho' - \rho)} \right]. \quad (68)$$

The parent dipole remains unchanged.

The equivalent BK equation for this model reads

$$\frac{\partial}{\partial y} Z(\rho, y|u) = \bar{\alpha} Z(\rho, y|u) \int_0^{+\infty} d\rho' \frac{dp}{dy}(\rho \rightarrow \rho') [Z(\rho', y|u) - 1]. \quad (69)$$

The eigenfunctions of the kernel are $e^{-\gamma\rho}$, and the characteristic function is

$$\bar{\alpha}\chi(\gamma) = \bar{\alpha} \left(\frac{1}{\gamma} + \frac{1}{1-\gamma} \right). \quad (70)$$

¹⁰The diffusive approximation is however well-justified for the evolution of the gluon density at a fixed impact parameter, as was previously documented (see e.g. Ref. [29, 30]).

¹¹Note that with the full two-dimensional transverse space, the natural variable is $\rho = \ln x_{01}^2/r^2$.

One gets the double-log limit by simply turning off the splittings to larger dipoles (namely by leaving out the second term in the probability density $\frac{dp}{dy}(\rho \rightarrow \rho')$ in Eq. (68).) On the other hand, the infrared cutoff that models confinement is implemented by simply removing dipoles created with a size larger than some given size of the same order as the size of the initial dipole.

We run the Monte Carlo event generator starting from a single dipole in the three configurations we study in this paper: full BFKL, BFKL with an infrared cutoff, and DL limit. We compare the numerical results to the analytical formulae (50), (57) and (34). More precisely, we use the following parametrizations:

$$\bar{n}P_n = N \times \begin{cases} \frac{\bar{n}}{n} e^{-\ln^2 n / (4\bar{\alpha}y)} & \text{for full BFKL,} \\ \frac{2}{c_{\text{DL}}} \left(\frac{n}{c_{\text{DL}}\bar{n}} - 1 \right) e^{-n/(c_{\text{DL}}\bar{n})} & \text{for the DL limiting model,} \\ \frac{1}{c} e^{-n/(c\bar{n})} & \text{for BFKL supplemented with a cutoff.} \end{cases} \quad (71)$$

The plot in Fig. 4 shows the numerical result for the following parameters: $\bar{\alpha}y = 2.5$ and $\rho_s = \ln x_{01}/r_s = 5$. The fits are performed for all numerical data points in the range $n/\bar{n} \geq 2$. We see that the matching with the analytical formulae is very good, except, unsurprisingly, for small values of n/\bar{n} ($\sim \mathcal{O}(1)$). Since full BFKL does not obey KNO scaling, the value of \bar{n} is needed in that case: We take it as an output of the Monte Carlo, $\bar{n} = 3231$. We get the following determination of the parameters:

- BFKL: $N = 462$,
- DL: $N = 0.85$,
- BFKL with a cutoff: $N = 1.82$, $c = 0.70$.

The unnaturally large value of the normalization N in the case of the BFKL fit is due to the fact that we have neglected potentially large but slowly varying factors in the argument of the exponential (see Eq. (50)), of the form $\ln n \times \ln \ln n$.

We have not been able to test numerically the universality of c and the dependence of the prefactor in the BFKL case upon the dipole size. This would require the use of a Monte Carlo that includes the full QCD dynamics, such as the one developed in Ref. [31], and to run it in a large enough range of values of y and ρ .

References

- [1] F. Gelis and B. Schenke, to appear in Annual Reviews of Nuclear and Particle Science, arXiv:1604.00335 [hep-ph].
- [2] B. Alver, M. Baker, C. Loizides and P. Steinberg, arXiv:0805.4411 [nucl-ex].
- [3] L. McLerran and M. Praszalowicz, Annals Phys. **372**, 215 (2016) doi:10.1016/j.aop.2016.05.010 [arXiv:1507.05976 [hep-ph]].
- [4] A. Dumitru, E. Iancu, L. Portugal, G. Soyez and D. N. Triantafyllopoulos, JHEP **0708**, 062 (2007) doi:10.1088/1126-6708/2007/08/062 [arXiv:0706.2540 [hep-ph]].
- [5] F. Gelis, R. B. Peschanski, G. Soyez and L. Schoeffel, Phys. Lett. B **647**, 376 (2007) doi:10.1016/j.physletb.2007.01.055 [hep-ph/0610435].

- [6] H. Mäntysaari and B. Schenke, Phys. Rev. Lett. **117** (2016) 052301, doi:10.1103/PhysRevLett.117.052301
- [7] J. P. Blaizot, private communication.
- [8] L. N. Lipatov, Sov. J. Nucl. Phys. **23**, 338 (1976) [Yad. Fiz. **23**, 642 (1976)].
- [9] E. A. Kuraev, L. N. Lipatov and V. S. Fadin, Sov. Phys. JETP **45**, 199 (1977) [Zh. Eksp. Teor. Fiz. **72**, 377 (1977)].
- [10] I. I. Balitsky and L. N. Lipatov, Sov. J. Nucl. Phys. **28**, 822 (1978) [Yad. Fiz. **28**, 1597 (1978)].
- [11] A. H. Mueller, Nucl. Phys. B **415**, 373 (1994).
- [12] A. H. Mueller, “Multiplicity Fluctuations in Proton Nucleus Collisions”, communication at the workshop “*Ab Initio Approaches in many-body QCD confront Heavy-Ion Experiments*”, Heidelberg, December 15, 2014, unpublished.
- [13] E. Iancu, A. H. Mueller and S. Munier, Phys. Lett. B **606**, 342 (2005) doi:10.1016/j.physletb.2004.12.009 [hep-ph/0410018].
- [14] A. H. Mueller and S. Munier, Phys. Lett. B **737**, 303 (2014) doi:10.1016/j.physletb.2014.08.058 [arXiv:1405.3131 [hep-ph]].
- [15] S. Munier, Phys. Rept. **473**, 1 (2009) doi:10.1016/j.physrep.2009.02.001 [arXiv:0901.2823 [hep-ph]].
- [16] S. Munier, Sci. China Phys. Mech. Astron. **58**, no. 8, 81001 (2015) doi:10.1007/s11433-015-5666-7 [arXiv:1410.6478 [hep-ph]].
- [17] Y. V. Kovchegov and E. Levin, “Quantum chromodynamics at high energy,” Cambridge Monographs on Particle Physics, Nuclear Physics and Cosmology, Cambridge University Press, 2012.
- [18] Y. V. Kovchegov and A. H. Mueller, Nucl. Phys. B **529**, 451 (1998) doi:10.1016/S0550-3213(98)00384-8 [hep-ph/9802440].
- [19] A. H. Mueller, arXiv:1607.05623 [hep-ph].
- [20] I. Balitsky, Nucl. Phys. B **463** (1996) 99–160.
- [21] Y. V. Kovchegov, Phys. Rev. D **60** (1999) 034008.
- [22] Y. L. Dokshitzer, V. S. Fadin and V. A. Khoze, Z. Phys. C **18**, 37 (1983).
- [23] Y. L. Dokshitzer, V. A. Khoze, A. H. Mueller and S. I. Troian, “Basics of perturbative QCD,” Gif-sur-Yvette, France: Ed. Frontieres (1991) 274 p.
- [24] Z. Koba, H. B. Nielsen and P. Olesen, Nucl. Phys. B **40**, 317 (1972). doi:10.1016/0550-3213(72)90551-2
- [25] G. P. Salam, Nucl. Phys. B **449**, 589 (1995) [hep-ph/9504284].
- [26] T. Lappi and L. McLerran, Nucl. Phys. A **772**, 200 (2006) doi:10.1016/j.nuclphysa.2006.04.001 [hep-ph/0602189].

- [27] F. Gelis, T. Lappi and L. McLerran, Nucl. Phys. A **828** (2009) 149 doi:10.1016/j.nuclphysa.2009.07.004 [arXiv:0905.3234 [hep-ph]].
- [28] A. Doche, Master's thesis report, École polytechnique, 2013.
- [29] S. Munier, G. P. Salam and G. Soyez, Phys. Rev. D **78**, 054009 (2008) doi:10.1103/PhysRevD.78.054009 [arXiv:0807.2870 [hep-ph]].
- [30] A. H. Mueller and S. Munier, Phys. Rev. D **81**, 105014 (2010) doi:10.1103/PhysRevD.81.105014 [arXiv:1002.4575 [hep-ph]].
- [31] G. P. Salam, Comput. Phys. Commun. **105**, 62 (1997) doi:10.1016/S0010-4655(97)00066-0 [hep-ph/9601220].